Zeitschrift für Kristallographie, Bd. 141, S. 31—58 (1975)

Study of the force field of scheelite

By **Kazuaki Iishi**

Department of Mineralogical Sciences and Geology,
Faculty of Literature and Science, Yamaguchi University

(Received 11 September 1972 and in revised form 31 December 1973)

Auszug

Die Methode der G- und F-Matrizen wurde zum Studium des Kraftsystems in Scheelit angewendet. Die Aufspaltung der intramolekularen Schwingungen und die Gitterschwignungen werden beide durch die interatomaren Wechselwirkungen erklärt. Die erhaltenen interatomaren Kraftkonstanten von nichtgebundenen Sauerstoffpaaren in Scheelit folgen näherungsweise einem 6-12-Lennard-Jones-Ansatz. Behandlung mit Normalkoordinaten liefert eine vollständige Diskussion der intramolekularen Normalschwingungen und der Gitterschwingungen.

Für das tetraedrische Ion WO_4^{2-} (Symmetrie T_d) erfolgt die Schwingung $\nu_2\ (E)$ bei höherer Frequenz als die Schwingung $\nu_4\ (F_2)$, entgegen dem üblichen Verhalten. Dies wird erläutert durch Berechnung und Vergleich der Normalschwingungen und der Schwingungsformen verschiedener Arten tetraedrischer Ionen wie SiO_4^{4-}, PO_4^{3-}, SO_4^{2-}, MoO_4^{2-} und WO_4^{2-}. Die Zuordnung der Schwingungen wird auch theoretisch bestätigt.

Abstract

The G and F matrix method has been applied to the study of the force field of scheelite. The splitting of the intramolecular vibration bands and the lattice vibrations have been clarified at the same time through the intermolecular atom-atom interactions. The obtained interatomic force constants of nonbonded oxygen pairs in scheelite follow roughly the Lennard-Jones 6-12 law. The normal modes of the intramolecular vibrations and the lattice vibrations have been fully discussed on the basis of the normal-coordinate treatment.

For the tetrahedral ions (T_d symmetry) of the WO_4^{2-}, $\nu_2(E)$ is larger than $\nu_4(F_2)$, representing an opposite relation to the usual order. This has been explained by calculating and comparing the normal vibration and the modes of vibration for several kinds of the tetrahedral ions such as SiO_4^{4-}, PO_4^{3-}, SO_4^{2-}, MoO_4^{2-} and WO_4^{2-}. The assignment of the vibrations has also been theoretically confirmed.

Introduction

The infrared and Raman spectroscopies are generally thought to be the most useful method for analyzing the characteristics of the crystals. To obtain certain information with respect to the forces controlling the crystal structure or to determine the interatomic or interionic forces in the lattice through calculation of the frequencies the spectroscopies play an important role. Recent progress in the study of the lazer Raman spectroscopy and of the far-infrared interferometry makes it possible to analyse the comparatively complicated structures of anisotropic crystals using the method of polarized radiation. Large values of the magnitude of splitting are found in experiments of scheelite.

In the present paper the G and F matrix method has been applied to the crystals under consideration and the results derived are compared with the observed values of the intramolecular vibration splitting and lattice frequency. This result gives important informations regarding the interatomic forces of this crystal. The dynamics of the molecules and ions in the crystalline environment have been examined by comparing their state in the crystals with their behaviors in free conditions.

I. The tetrahedral ions

First, the molecules in an isolated state without being affected by the surrounding conditions such as the neighbors, the crystalline environment and so on are disputed. The molecule in question is classified into the point group T_d. Its symmetry species and characters are given in Table 1.

As its potential function, the Urey-Bradley force field (SHIMANOUCHI, 1963) was used as follows:

$$V = \tfrac{1}{2}\Sigma K_i (\varDelta r_i)^2 + \tfrac{1}{2}\Sigma H_{ij} r_i r_j (\varDelta \alpha_{ij})^2 + \tfrac{1}{2}\Sigma F_{ij} (\varDelta q_{ij})^2$$

$$+ \tfrac{1}{2}\varkappa \qquad \text{(terms due to internal tensions).}$$

Here K, H and F are the stretching, bending and repulsive force constants, respectively. The first-order repulsive force constant F' is estimated $-0.1\ F$.

The calculated values of frequency were converged to those observed through the least-squares method presented by SHIMANOUCHI and SUZUKI (1964). The measure of fitness (S) and the dispersions of force constants (σ_i) were calculated. The displacement of each atom

Table 1. *Character table for T_d symmetry*

T_d	E	$8C_3$	$6\sigma_d$	$6S_4$	$3C_2$	N_i	T_i	T_i'	R_i'	n_i	Infrared	Raman
A_1	1	1	1	1	1	1	0	0	0	1	f	$\alpha_{xx} + \alpha_{yy} + \alpha_{zz}$
A_2	1	1	—1	—1	1	0	0	0	0	0	f	f
E	2	—1	0	0	2	1	0	0	0	1	f	$\alpha_{xx} + \alpha_{yy} - 2\alpha_{zz}, \alpha_{xx} - \alpha_{yy}$
F_1	3	0	—1	1	—1	1	0	0	1	0	f	f
F_2	3	0	1	—1	—1	3	1	0	0	2	M_x, M_y, M_z	$\alpha_{xy}, \alpha_{yz}, \alpha_{xz}$

f: forbidden, N_i: number of degrees of freedom related to the ith species, T_i: number of over-all translations of the Bravais unit cell, T_i': number of the translational lattice modes, R_i': number of the rotational lattice modes, n_i: number of the normal modes of the intramolecular vibration.

in vibration is describable in terms of the transformation matrix L_x from the Cartesian coordinates X to the normal coordinates Q:

$$X = L_x Q \tag{1}$$

and calculated as the eigenvector for $M^{-1} F_x$ matrix:

$$M^{-1} F_x L_x = L_x \Lambda . \tag{2}$$

In this paper, the values for the optically active frequency were calculated on the basis of the mass-adjusted Cartesian symmetry coordinate (MANN *et al.*, 1954). Since the mass-adjusted Cartesian displacement is physically more significant, L_{xm} is calculated as follows:

$$X_m = M^{1/2} X , \tag{3}$$

$$X_m = L_{xm} Q , \tag{4}$$

$$L_{xm} = M^{1/2} L_x . \tag{5}$$

Results

The calculated and observed values (MÜLLER and KREBS, 1967) of frequency, the determined force constants and the Jacobian matrix for WO_4^{2-}, MoO_4^{2-}, SO_4^{2-}, PO_4^{3-} and SiO_4^{4-} free ions are shown in Table 2. It is remarkable that the observed data coincide with the calculated ones. The weighed sum of the squared deviations S and the dispersion of the force constants σ are nearly equal to zero. L_{xm} matrix derived from the determined set of the force constants is aligned in Table 3. The modes of vibration for ν_1 and ν_2 are the same in the case of each tetrahedral ion as there is no relation to the central atom of the tetra-

Table 2. *Calculated and observed values of frequency* (cm^{-1}), *force constants* and Jacobian matrix of some* XO_4 *type ions with* T_d *symmetry*

SiO_4^{4-} free ion

Species		Frequencies		Force constants			
		Obs.	Calc.	K 3.7135	H 0.1918	F 0.6523	$\varkappa$ 0.6641
A_1	ν_1	819	819	0.063	0	0.25	0
E	ν_2	340	340	0	0.188	0.075	—0.025
F	ν_3	906	906	0.108	0.116	0.042	0.047
	ν_4	527	527	0.001	0.199	0.102	0.080

* Dimension of force constants is mdyn/Å for K, H and F, and mdyn · Å for $\varkappa$.

Table 2. *(Continued)*

PO_4^{3-} free ion

Species		Frequencies		Force constants			
		Obs.	Calc.	K 5.0090	H 0.2983	F 0.8211	$\varkappa$ 0.4862
A_1	ν_1	938	938	0.063	0	0.25	0
E	ν_2	420	420	0	0.188	0.075	−0.028
F	ν_3	1 017	1 017	0.105	0.089	0.046	0.040
	ν_4	567	567	0	0.208	0.097	0.093

SO_4^{2-} free ion

Species		Frequencies		Force constants			
		Obs.	Calc.	K 6.0338	H 0.4203	F 0.7686	$\varkappa$ 0.5745
A_1	ν_1	983	983	0.063	0	0.25	0
E	ν_2	450	450	0	0.188	0.075	−0.030
F	ν_3	1 105	1 105	0.103	0.094	0.043	0.045
	ν_4	611	611	0.001	0.198	0.098	0.094

MoO_4^{2-} free ion

Species		Frequencies		Force constants			
		Obs.	Calc.	K 4.7263	H 0.1532	F 0.7018	$\varkappa$ −0.1815
A_1	ν_1	894	894	0.063	0	0.25	0
E	ν_2	381	381	0	0.188	0.075	−0.023
F	ν_3	833	833	0.076	0.004	0.072	0.001
	ν_4	318	318	0.001	0.177	0.058	0.065

WO_4^{2-} free ion

Species		Frequencies		Force constants			
		Obs.	Calc.	K 5.0336	H 0.1213	F 0.7841	$\varkappa$ −0.0183
A_1	ν_1	931	931	0.063	0	0.25	0
E	ν_2	373	373	0	0.188	0.075	−0.022
F	ν_3	833	833	0.069	0	0.079	0
	ν_4	320	320	0.001	0.154	0.049	0.055

Table 3. L_{xm} *matrix of some* XO_4 *tetrahedral ions*

	SiO_4^{4-}				PO_4^{3-}		SO_4^{2-}		MoO_4^{2-}		WO_4^{2-}	
	ν_1	ν_2	ν_3	ν_4	ν_3	ν_4	ν_3	ν_4	ν_3	ν_4	ν_3	ν_4
x_1	0	0	−0.58	−0.35	−0.55	−0.38	−0.56	−0.37	−0.31	−0.41	−0.23	−0.35
y_1	0	0	0	0	0	0	0	0	0	0	0	0
z_1	0	0	−0.41	−0.25	−0.39	−0.27	−0.39	−0.26	−0.22	−0.29	−0.16	−0.25
x_2	0	0.5	0.04	0.36	0.03	0.37	0.04	0.37	−0.04	0.43	−0.05	0.45
y_2	0	0	0	0	0	0	0	0	0	0	0	0
z_2	0.5	0	0.35	−0.27	0.37	−0.24	0.36	−0.25	0.46	−0.07	0.48	−0.01
x_3	0.47	0.17	0.34	−0.13	0.36	−0.10	0.36	−0.11	0.42	0.08	0.43	0.14
y_3	0	0	0	0	0	0	0	0	0	0	0	0
z_3	−0.17	0.47	−0.43	0.43	−0.10	0.43	−0.08	0.43	−0.19	0.42	−0.21	0.43
x_4	−0.24	−0.33	0.19	0.12	0.19	0.13	0.20	0.13	0.19	0.25	0.19	0.30
y_4	−0.41	0.29	0.26	−0.43	0.29	−0.41	0.27	−0.42	0.40	−0.30	0.42	−0.27
z_4	−0.17	−0.24	0.14	0.08	0.14	0.09	0.14	0.09	0.13	0.18	0.14	0.21
x_5	−0.24	−0.33	0.19	0.12	0.19	0.13	0.20	0.13	0.19	0.25	0.19	0.30
y_5	0.41	−0.29	−0.26	0.43	−0.29	0.41	−0.27	0.42	−0.40	0.30	−0.42	0.27
z_5	−0.17	−0.24	0.14	0.08	0.14	0.09	0.14	0.09	0.13	0.18	0.14	0.21

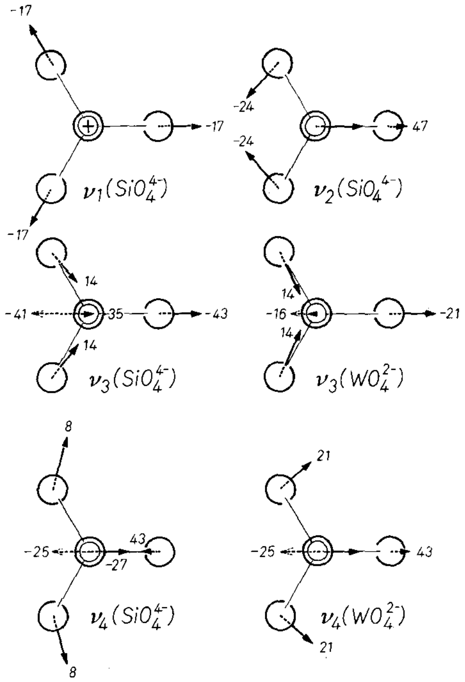

Fig. 1. Modes of vibration for the tetrahedral XY_4 ion (SiO_4^{4-} and WO_4^{2-})

hedron. The L_{xm} data of ν_1 and ν_2 are given only in relation to SiO_4^{4-}. In the case of SiO_4^{4-} and WO_4^{2-}, the displacement vectors along x, y, and z axes of each atom are illustrated in Fig. 1. Here the data of L_{xm} matrix are used for each frequency.

Discussion

A) The assignment of vibration bands

The assignment of $\nu_2(E)$ of WO_4^{2-} ion was ambiguous to its very low intensity. Busey and Keller (1964) assigned correctly this vibration band by examing the infrared spectra of Na_2WO_4 (crystal) bearing a spinel structure with the site symmetry T_d. According to their results, for the tetrahedral ion of WO_4^{2-} $\nu_2(E) > \nu_4(F_2)$ and $\nu_1(A_1) > \nu_3(F_1)$, which represents an inversion of the usual order for the tetrahedral ions such as SO_4^{2-}, PO_4^{3-} and SiO_4^{4-} *etc*. These inversion of frequency of ν_2 and ν_4 or ν_1 and ν_3 are explained below from the viewpoint of the obtained modes of vibration and the obtained Jacobian matrix.

a) The relation $\nu_1 \gtrless \nu_3$

As far as SiO_4^{4-} is concerned, the Jacobian matrix of the force constants K, H and $\varkappa$ are fairly large for ν_3 compared with ν_1. On the other hand, the force constant F has a stronger effect upon ν_1 than upon ν_3, but the absolute value of K is very large. Consequently the frequency values of ν_3 becomes larger than that of ν_1. Different effects of each force constant on frequency are clarified through examination of the modes of vibration shown in Fig. 1. On account of the displacement of oxygen only along Si—O bond vectors, a distortion of the angle is not derived from the change of each atom and hence the force constants K and F only affect ν_1 as the potential energy. In the case of ν_3 the Si atom also moves as oxygen atom and therefore the force constant K gives the effect largely on ν_3 than ν_1. Distorsion of the angle O—Si—O is ascribed to the displacement of Si atom. Thus the force constants H and $\varkappa$ influence ν_3 differently from ν_1. In the case of ν_3, the displacement of the central atom of tetrahedron diminishes the value of the Jacobian matrix of the repulsive force F.

In the case of WO_4^{2-} ion, the displacement vector of the tungsten atom in ν_3 is less than that of the silicon atom in the case of SiO_4^{4-} (Fig. 1). It thus results that the values of the Jacobian matrix of the force constants K, H and $\varkappa$ of ν_3 are nearly equal to those of ν_1. Whether ν_1 is larger than ν_3 or not, therefore, may be determined by the value of the Jacobian matrix of the repulsive force constant F. Inspection of Table 2 suggests that the repulsive force affects rather ν_1 than ν_3, and therefore ν_1 is larger than ν_3.

b) The relation $\nu_2 \gtrless \nu_4$

The mode of ν_4 vibration of WO_4^{2-} with the oxygen atoms vibrating in the direction nearly perpendicular the edge of the tetrahedron apparently differs from that for SiO_4^{4-} with the oxygen atoms vibrating nearly along the edges of tetrahedron. The values of the Jacobian matrix related to the repulsive force constant F for ν_4 is larger than that for ν_2 in the case of SiO_4^{4-}. The effect of the repulsive force constant F for ν_4 is less than that for ν_2 in the case of WO_4^{2-}. However the inverse relation of ν_4 and ν_2 is most effectively influenced by the value of the internal molecular tension $\varkappa$. As is shown in Table 2, the tetrahedral ions such as SiO_4^{4-}, PO_4^{3-}, SO_4^{2-} *etc.* indicate the relatively large value of $\varkappa$ whereas their central atoms are rather less in weight. On the other hand, the values of $\varkappa$ in the case of the tetrahedra of WO_4^{2-} and

MoO_4^{2-} *etc.* with the heavy central atoms are very small or negative. Moreover, the Jacobian matrix of $\varkappa$ has a negative value for ν_2 and a positive value for ν_4. Because of this situation, ν_4 is larger than that of ν_2 for SiO_4^{4-}, PO_4^{3-} and SO_4^{2-} *etc.* and vice versa for WO_4^{2-} and MoO_4^{2-} *etc.*

B) The repulsive force constant and the interatomic distance

The Lennard-Jones type of the potential is:

$$U = -A'/r^6 + B'/r^{12}, \tag{6}$$

where U is the potential energy, A' and B' the constants for the attractive and repulsive terms respectively, and r the interatomic distance. The non-bonded force constant F is given as:

$$F = d^2U/dr^2 = -42\,A'/r^8 + 156\,B'/r^{14} = -A/r^8 + B/r^{14}. \tag{7}$$

Based on this assumption, Levitt (1969) obtained 231 mdyn · Å^7 for A and 530,000 mdyn · Å^{13} for B through site-group analysis in the case of fluorapatite. If these values are now valid, 1.89, 1.16, 0.55, 0.26 and 0.22 mdyn/Å are obtained for SO_4^{2-}, PO_4^{3-}, SiO_4^{4-}, MoO_4^{2-} and WO_4^{2-} respectively, although these values are of course variable to some extent. The obtained repulsive force constants are very different from those obtained based on the assumption of the Lennard-Jones type of potential. Furthermore, there is no reasonable relation between the oxygen · · · oxygen distance and the repulsive force constants. The unreasonability of the obtained repulsive force constants can perhaps be solved by introducing another force constant $p(\Delta r, \Delta r')$ related bond-bond interaction. The addition of the correction term p to the Urey-Bradley force field, however, amounts to five of the force constants to be determined, whereas four kinds of the fundamental frequency can be observed. This problem will be discussed after the site-group and factor-group analyses of scheelite.

II. The site-symmetry treatment of scheelite

A) The observed data

The values of frequency for the infrared active vibrations have been determined by Barker (1964) through measurement of the infrared reflectivity of single crystals. The species B_u inactive for infrared

Table 4. *Internal vibrations of the tungstate ion in scheelite* (cm^{-1})

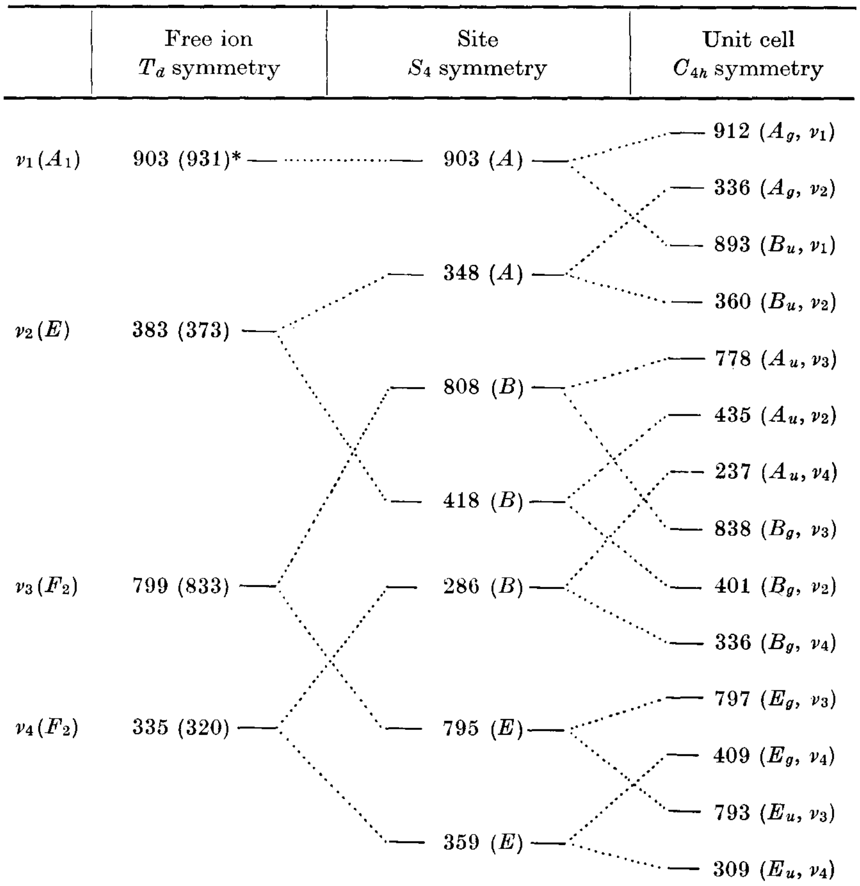

* The values of frequency in parentheses are solution data from BUSEY and KELLER (1964).

Table 5. *External vibrations in scheelite*

Rotatory		Translatory	
A_g	218 cm^{-1}	B_g	84 cm^{-1}
B_u	213	B_g	210
E_g	275	A_u	180
E_u	202	E_g	117
		E_g	195
		E_u	143

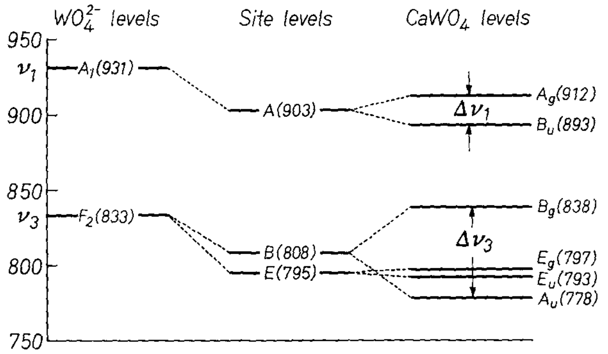

Fig. 2*a*. Internal mode in $CaWO_4$

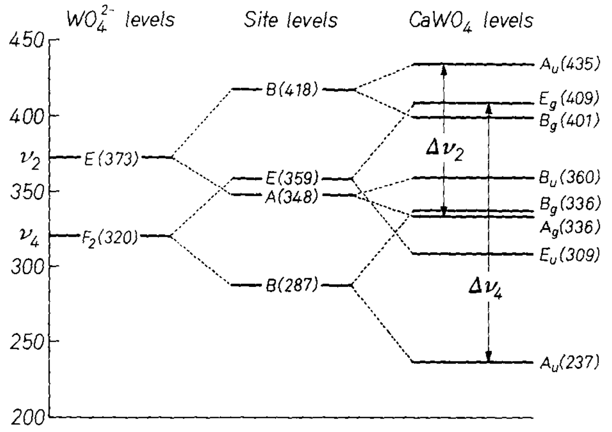

Fig. 2*b*. Internal mode in $CaWO_4$

and Raman are assigned on the basis of their infrared active data under the condition of the sheared strain (Scott, 1968*a*). The Raman spectra were investigated by Russell and Loudon (1965), Porto and Scott (1967), and Khanna *et al.* (1968). As has been stated already in the tetrahedral ion section, $\nu_2(A_u)$ and $\nu_4(A_u)$ together with $\nu_2(B_g)$ and $\nu_4(B_g)$ were often misassigned. The data of the frequency o scheelite were reassigned by Scott (1968 *b*) based on the data given by Porto and Scott for the Raman effect and those given by Barker for the infrared absorption. This paper is based on the assignment given by Scott.

The observed values of the internal and external vibration in association with the assignment are listed in Tables 4 and 5. The values of the frequency for the infrared and Raman are averaged to obtain the data of the site-group analysis. The complete scheme of the vibration level for $CaWO_4$ is given in Figs. 2*a* and 2*b*, showing the observed splitting of the crystal field and some of the degeneracies of frequency for the free ions.

B) Calculation

A normal-coordinate analysis of the WO_4^{2-} group in scheelite has been carried out based on the molecular parameters (Table 6) calculated from x-ray data (ZALKIN and TEMPLETON, 1964). The symmetry elements are one fourfold rotation-reflection axis, S_4, and two twofold axes. The present analysis is related to an XY_4 molecule with S_4 symmetry similar to that revealed in Fig. 3. The character table is shown in Table 7.

The angle α on the side of the S_4 axis is slightly larger than the angle β lying skew to the same axis. It thus follows that in this molecules the bending force constants H_α and H_β and the repulsive force constants F_α and F_β are added to the stretching-force constant K and the internal tension $\varkappa$.

Table 6. *Molecular parameters used in calculation of the values of frequency of* WO_4^{2-} (S_4-site symmetry)

$r(W—O)[1,2]$	1.788 Å	$\alpha(O—W—O)[3,1,5]$	113°27′
$q_\alpha(O\cdots O)[3,5]$	2.985 Å	$\beta(O—W—O)[2,1,3]$	107°56′
$q_\beta(O\cdots O)[2,3]$	2.880 Å		

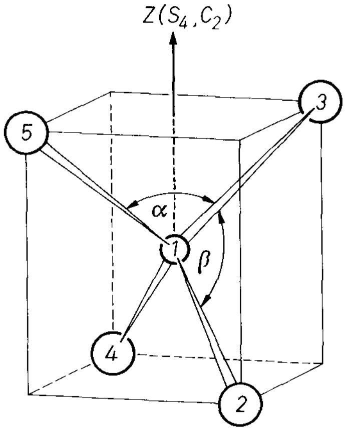

Fig. 3. Schematic representation of the WO_4^{2-} ion with S_4 symmetry

Table 7. *Symmetry species and the characteristics of the* WO_4^{2-} *ion in the scheelite structure**

S_4	E	S_4	C_2	S_4^3	N_i	T_i	T'_i	R'_i	n_i	Infrared	Raman
A	1	1	1	1	3	0	0	1	2	f	$\alpha_{xx}+\alpha_{yy}$, α_{zz}
B	1	-1	1	-1	4	1	0	0	3	M_z	$\alpha_{xx}-\alpha_{yy}$, α_{xy}
E	1 1	i $-i$	-1 -1	$-i$ i	4	1	0	1	2	(M_x, M_y)	$(\alpha_{yz}, \alpha_{zx})$

* The notation is the same as is given in Table 1.

Results and discussion

The results of the calculated frequency and the force constants together with their Jacobian matrix are shown in Table 8. The coincidence of the observed values of frequency with the calculated ones is considered as very good. The weighted sum of squared deviations S is estimated 0.00012, the average of frequency deviation 0.6% and the maximum deviation 3.9 cm^{-1} respectively. On the basis of these force constants determined in set I the frequency variation and the frequency splitting from T_d symmetry to S_4 site symmetry are clarified as follows.

The values of ν_2 and ν_4 are regulated mainly by bending-force constant for the O—W—O angle and the repulsive-force constant for

Table 8. *Calculated and observed values of frequency* (cm^{-1}), *force constants* and Jacobian matrix of* WO_4^{2-} *ion in scheelite*

Species		Frequencies		Force constants					
		Obs.	Calc.	K 4.580	H_α 0.0328	F_α 0.8243	H_β 0.2181	F_β 0.7505	$\varkappa$ 0.0306
A	ν_1	903	903.2	0.062	0	0.088	0	0.162	0
	ν_2	348	350.4	0	0.125	0.045	0.058	0.025	-0.020
B	ν_3	808	804.8	0.068	0	0.094	0	-0.009	0
	ν_2	418	414.1	0	0	0	0.192	0.080	-0.021
	ν_4	286	284.9	0.001	0.155	0.044	0	0	0.052
E	ν_3	795	797.9	0.069	0	-0.004	0	0.082	0
	ν_4	359	361.1	0.001	0	0	0.153	0.050	0.051

* Dimension of force constants is mdyn/Å for K, H, and F, and mdyn · Å for $\varkappa$.

Table 9. *Calculated and observed values of frequency* (cm^{-1}) *and force constants* of* WO_4^{2-} *in scheelite*

	Set I	Set II	Set III
K	4.5830 ± 0.0720	6.2835 ± 0	5.8502 ± 0.0447
H_α	0.0328 ± 0.0172	0.3341 ± 0	0.3130 ± 0.0045
F_α	0.8243 ± 0.0519	-0.0261 ± 0	0.0832 (fixed)
H_β	0.2181 ± 0.0149	0.6602 ± 0	0.4802 ± 0.0046
F_β	0.7505 ± 0.0378	-0.3059 ± 0	0.1484 (fixed)
$\varkappa$	0.0306 ± 0.0134	-0.0214 ± 0	-0.0401 ± 0.0127
p		0.7424 ± 0	0.5021 ± 0.0277

	Obs.	Calc.	Deviation	Calc.	Deviation	Calc.	Deviation
A	903 cm^{-1}	903.2 cm^{-1}	0 %	903.0 cm^{-1}	0 %	903.0 cm^{-1}	0 %
	348	350.4	0.7	348.0	0	349.8	0.5
B	808	804.8	−0.4	808.0	0	795.1	−1.6
	418	414.1	−0.9	418.0	0	415.0	−0.7
	286	284.9	−0.4	286.0	0	285.2	−0.3
E	795	797.9	0.4	795.0	0	806.9	1.5
	359	361.1	0.6	359.0	0	360.6	0.5
Root-mean-square deviation		0.5		0		0.9 %	
Weighted sum of squared deviations		0.00012		0		0.00033	

* Dimension of force constants is mdyn/Å for K, H, F and p, and mdyn · Å for $\varkappa$.

the O···O non-bonded oxygen atom. The latter value in the site symmetry S_4 ($F_\alpha = 0.7732$ mdyn/Å and $F_\beta = 0.7545$ mdyn/Å) is nearly equal to that in the free ion (0.7841 mdyn/Å). Furthermore, $\nu_2(A$, 348 $cm^{-1})$ and $\nu_4(B$, 286 $cm^{-1})$ are mainly in relation to H_α regarding the bending-force constant in contrast to $\nu_2(B$, 418 $cm^{-1})$ and $\nu_4(E$, 359 $cm^{-1})$ concerned mainly with H_β. That the values in the former case are smaller than those in the latter is attributed to $H_\alpha < H_\beta$. The average of H_α(0.0328 mdyn/Å) and H_β(0.2181 mdyn/Å) in the site symmetry is nearly equal to the value of H (0.1213 mdyn/Å) in the free ion.

As far as the frequency variation and the frequency splitting from T_d symmetry to S_4 site symmetry are concerned, the explanation given above is believed qualitatively correct. As referred to already, the values of non-bonded force constants ($F_\alpha = 0.8243$ and $F_\beta = 0.7505$ mdyn/Å) are however unreasonably highly estimated with those obtained by introducing 231 mdyn · Å^7 for A and 530,000 mdyn · Å^{13} for B, respectively, to the Lennard-Jones potential expressed in equation (7), wherefrom F_α and F_β are calculated as 0.0832 and 0.1484 mdyn/Å respectively. The bond-bond interaction potential p is considered as the correction term in set II. The calculated values of the frequency well coincide with those observed, as shown in Table 9. However, the values of the non-bonded force constants ($F_\alpha = -0.0261$ mdyn/Å and $F_\beta = -0.3059$ mdyn/Å) are negative and accordingly unreasonable. In set III, therefore, the non-bonded force constants F_α and F_β are tentatively fixed as 0.0832 and 0.1484 mdyn/Å respectively. The coincidence of the observed values of the frequency with those calculated is quite acceptable though a little worse than in the set I and set II. The force constants of set III are physically reasonable differing from the other cases.

It should be borne in mind here that the neglect of the lattice effects and other interaction force constants have some influences both on the magnitude of the derived force constants and on the trends which they follow. The factor-group method is most effective to treat the behavior of the vibration of the crystals concerned. Therefore the perfect factor-group analysis is adopted on the basis of the treatment related to the Bravais unit cell for clarifying the relationship between the observed band splitting and the lattice frequency. The analysis gives the information about the intermolecular forces as is shown in the following.

III. The factor-group treatment of scheelite

The unit cell of $CaWO_4$ belonging to the space group C_{4h}^6 contains four molecules. The crystal structure of scheelite has been refined on the basis of x-ray diffraction data for its single crystal by Zalkin and Templeton (1964) and of the neutron diffraction data by Kay *et al.* (1964), the results of which are in excellent agreement. The b axis projection of the unit cell in question is illustrated in Fig. 4.

The primitive or Bravais cell is defined as the smallest unit in which each pair of two atoms become nowhere equivalent. In this case, Bravais unit cell contains only two $CaWO_4$ "molecules" or 12 atoms. The selection rule is deducible from the symmetry in the corresponding point group C_{4h}. Six species of symmetry are given in

Table 10. The modes are dividable into the "internal" and the "external" types and the latter furthermore into the "rotatory" and the "translatory" types.

The potential-energy matrix is constructed of the intramolecular potential and the intermolecular potential part. For the intramolecular potential of each molecule, the same potential used for the site-group analysis is assumed. For the intermolecular potential, we assumed quadratic potential for five kinds of O···O distances $q_1^{\mathrm{o\cdots o}}$, $q_2^{\mathrm{o\cdots o}}$, $q_3^{\mathrm{o\cdots o}}$, $q_4^{\mathrm{o\cdots o}}$ and $q_5^{\mathrm{o\cdots o}}$ which are smaller than 3.2 Å, one kind of W···W distances $q_1^{\mathrm{w\cdots w}}$ and of Ca···Ca distances $q_1^{\mathrm{ca\cdots ca}}$, two kinds of Ca—O distances $r_1^{\mathrm{ca-o}}$ and $r_2^{\mathrm{ca-o}}$ (set I, Fig. 4 and Table 11). The distances larger than those used in this treatment are not taken into consideration because the corresponding force constants are too small to give significant effect on the frequency of vibration.

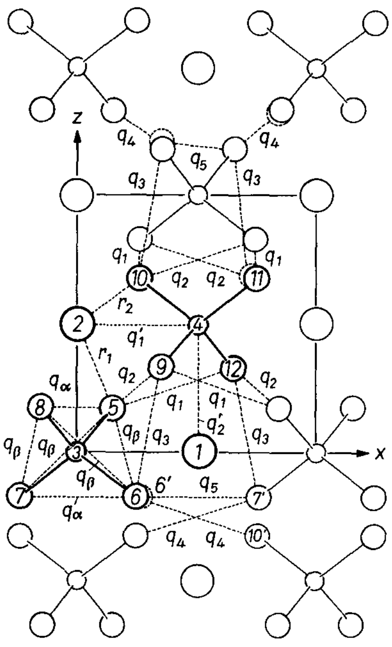

Fig. 4. Crystal structure of $CaWO_4$

As has frequently been assumed (Devlin, 1963, 1964), the attractive forces between the non-bonded atoms are not negligible. Thus, the functions of the bending and non-bonded force constants appear

Table 10. *The symmetry species and the characteristics of the scheelite structure**

C_{4h}	E	C_4	C_2	C_4^3	i	S_4^3	σ_h	S_4	N_i	T_i	T_i'	R_i'	n_i	Infrared	Raman
A_g	1	1	1	1	1	1	1	1	3	0	0	1	2	f	$\alpha_{xx} + \alpha_{yy}$, α_{zz}
B_g	1	—1	1	—1	1	—1	1	—1	5	0	2	0	3	f	$\alpha_{xx} - \alpha_{yy}$, α_{xy}
E_g	1 1	i $-i$	—1 —1	$-i$ i	1 1	i $-i$	—1 —1	$-i$ i	5	0	2	1	2	f	$(\alpha_{yz}, \alpha_{zx})$
A_u	1	1	1	1	—1	—1	—1	—1	5	1	1	0	3	M_z	f
B_u	1	—1	1	—1	—1	1	—1	1	3	0	0	1	2	f	f
E_u	1 1	i $-i$	—1 —1	$-i$ i	—1 —1	$-i$ i	1 1	i $-i$	5	1	1	1	2	(M_x, M_y)	f

* The notation is the same as is given in Table 1.

Table 11. *Molecular parameters used in calculation of frequency of scheelite*

$r(W\text{—}O)[3,5]$	1.788 Å	$q(W\cdots W)[3,4]$	3.868 Å
$r_1(Ca\text{—}O)[2,5]$	2.438	$q(Ca\cdots Ca)[1,2]$	3.868
$r_2(Ca\text{—}O)[2,10]$	2.479	$q_1(W\cdots Ca)[2,4]$	3.707
$q_\alpha(O\cdots O)[5,8]$	2.985	$q_2(W\cdots Ca)[1,4]$	3.868
$q_\beta(O\cdots O)[5,6]$	2.880	$\alpha(O\text{—}W\text{—}O)[5,3,8]$	113°27′
$q_1(O\cdots O)[5,12]$	2.767	$\beta(O\text{—}W\text{—}O)[5,3,6]$	107°56′
$q_2(O\cdots O)[5,9]$	2.874	$\phi_1(O\text{—}Ca\text{—}O)[5,1,12]$	68°30′
$q_3(O\cdots O)[6,9]$	2.938	$\phi_2(O\text{—}Ca\text{—}O)[6,1,9]$	73°24′
$q_4(O\cdots O)[6',10']$	3.036	$\phi_3(O\text{—}Ca\text{—}O)[6,1,10']$	76°18′
$q_5(O\cdots O)[6,7']$	3.142	$\phi_4(O\text{—}Ca\text{—}O)[6,1,7']$	80°8′

to be quite similar to each other and difficult to be separated. Therefore, the bending force constants h for the O—Ca—O angle deformation are taken into account in the second calculation (set II).

Results and discussion

The values of the force-constants for set I and set II are given in Table 12. The calculated values of frequency (ν_{calc}) together with the observed ones (ν_{obs}) are listed in Table 13. The fact is that the

Table 12. *Force constants of scheelite* (mdyn/Å)

	Set I	Set II
$K(W\text{—}O)$	5.330 (fixed)	5.350 (fixed)
$H_\alpha(O\text{—}W\text{—}O)$	0.163 ± 0.016	0.152 ± 0.015
$F_\alpha(O\cdots O)$	0.063 ± 0.040	0.071 ± 0.009
$H_\beta(O\text{—}W\text{—}O)$	0.225 ± 0.014	0.240 ± 0.012
$F_\beta(O\cdots O)$	0.145 ± 0.021	0.142 ± 0.016
$k_1(Ca\text{—}O)$	0.481 ± 0.011	0.353 ± 0.014
$k_2(Ca\text{—}O)$	0.049 ± 0.004	0.130 ± 0.011
$h_1(O\text{—}Ca\text{—}O)$	0 (fixed)	− 0.118 ± 0.008
$f_1(O\cdots O)$	0.207 ± 0.006	0.247 ± 0.012
$f_2(O\cdots O)$	0.189 ± 0.004	0.154 ± 0.011
$f_3(O\cdots O)$	0.071 ± 0.004	0.090 ± 0.013
$f_4(O\cdots O)$	0.010 ± 0.005	0.049 ± 0.024
$f_5(O\cdots O)$	− 0.062 ± 0.005	0.021 ± 0.011
$f(W\cdots W)$	0.005 ± 0.005	0 (fixed)
$f_1(Ca\cdots W)$	0.165 ± 0.007	0.161 ± 0.005
$f_2(Ca\cdots W)$	− 0.091 ± 0.009	0.065 ± 0.010
$f(Ca\cdots Ca)$	0.054 ± 0.002	0.032 ± 0.004
$\varkappa$*	0.004 ± 0.014	0.021 ± 0.008
$p(W\text{—}O, W\text{—}O)$	0.495 ± 0.025	0.493 ± 0.018

* Dimension of $\varkappa$ is mdyn · Å.

Table 13. *Observed and calculated values of frequency of scheelite*

	ν_{obs}	Set I ν_{calc}	Set II ν_{calc}
Intramolecular vibration			
A_g	912 (ν_1)	901 cm^{-1}	909 cm^{-1}
	336 (ν_2)	341	332
B_u	893 (ν_1)	903	894
	360 (ν_2)	357	367
B_g	838 (ν_3)	785	795
	401 (ν_2)	401	400
	336 (ν_4)	329	328
A_u	778 (ν_3)	781	774
	435 (ν_2)	420	430
	237 (ν_4)	240	242
E_g	797 (ν_3)	801	800
	409 (ν_4)	426	409
E_u	793 (ν_3)	789	789
	309 (ν_4)	305	306
Translatory vibration			
	210 (B_g)	215	209
	195 (E_g)	188	182
	180 (A_u)	177	173
	143 (E_u)	144	143
	117 (E_g)	117	122
	84 (B_g)	84	87
Rotatory vibration			
	275 (E_g)	268	268
	218 (A_g)	216	219
	213 (B_u)	214	217
	202 (E_u)	211	211

calculated data for both sets indicate the sufficient coincidence with observed ones except for $\nu_3(B_g$, 838 cm$^{-1})$. But the data for the set I are not suitable for the force field of scheelite since the oxygen $\cdots$ oxygen repulsive force constants are not physically reasonable. The physically significant relationship between the interatomic distance

Table 14. *Jacobian matrix*

	$K(W-O)$	$H_\alpha(O-W-O)$	$F_\alpha(O\cdots O)$	$H_\beta(O-W-O)$	$F_\beta(O\cdots O)$	$k_1(Ca-O)$	$k_2(Ca-O)$	$h_1(O-Ca-O)$
	5.350	0.152	0.071	0.240	0.142	0.353	0.130	− 0.118
$\nu_1(A_g,\ 912)$	0.062	0.000	0.087	0.000	0.163	0.030	0.014	*0.009*
$\nu_1(B_u,\ 893)$	0.062	0.000	0.085	0.000	0.165	0.029	0.015	*0.080*
$\nu_2(A_g,\ 336)$	0.000	0.112	0.041	0.052	0.023	*0.005*	0.026	*0.049*
$\nu_2(B_u,\ 360)$	0.000	0.103	0.040	0.048	0.018	*0.027*	0.048	*0.010*
$\nu_2(B_g,\ 401)$	0.000	0.020	0.005	0.166	0.069	*0.011*	*0.000*	*0.016*
$\nu_2(A_u,\ 435)$	0.000	0.016	0.006	0.155	0.064	*0.055*	*0.032*	*0.045*
$\nu_3(B_g,\ 838)$	0.069	0.003	0.080	0.000	− 0.009	0.032	0.013	*0.009*
$\nu_3(A_u,\ 778)$	0.069	0.002	0.083	0.000	− 0.010	0.026	0.015	*0.074*
$\nu_3(E_g,\ 797)$	0.070	0.000	− 0.004	0.003	0.071	0.025	0.015	*0.069*
$\nu_3(E_u,\ 793)$	0.070	0.000	− 0.004	0.002	0.072	0.027	0.013	*0.007*
$\nu_4(B_g,\ 336)$	0.000	0.102	0.043	0.018	0.007	*0.050*	0.027	0.010
$\nu_4(A_u,\ 237)$	0.000	0.127	0.046	0.028	0.012	*0.004*	0.028	0.032
$\nu_4(E_g,\ 409)$	0.000	0.000	0.000	0.139	0.057	0.021	0.007	*0.094*
$\nu_4(E_u,\ 309)$	0.000	0.000	0.000	0.150	0.059	0.019	0.015	*0.014*
$T'(B_u, 210)$	0.000	0.024	0.008	0.008	0.003	0.027	0.035	0.074
$T'(E_g, 195)$	0.000	0.000	0.000	0.000	0.000	0.006	0.019	0.025
$T'(A_u, 180)$	0.000	0.010	0.003	0.010	0.004	0.036	0.004	0.101
$T'(E_u, 143)$	0.000	0.000	0.000	0.002	0.000	0.003	0.059	0.063
$T'(E_g, 117)$	0.000	0.000	0.000	0.008	0.003	0.005	0.000	0.015
$T'(B_g,\ 84)$	0.000	0.006	0.002	0.000	0.000	0.000	0.003	0.011
$R'(E_g, 275)$	0.000	0.000	0.000	0.003	0.002	0.026	0.063	0.021
$R'(A_g, 218)$	0.000	0.013	0.006	0.006	0.001	0.028	0.022	0.002
$R'(B_u, 213)$	0.000	0.022	0.009	0.010	0.004	0.007	0.000	0.102
$R'(E_u, 202)$	0.000	0.000	0.000	0.000	0.000	0.035	0.018	0.008

Italics indicate the important terms for frequency splitting.

and the values of the force constants is nowhere establishable. On the other hand, the force constants in the set II are physically reasonable except h_1^{o-ca-o} with the negative value. For examining and improving the negative value of h_1^{o-ca-o}, the deformation force constants h_2^{o-ca-o}, h_3^{o-ca-o} and h_4^{o-ca-o} (see Table 11) were furthermore introduced, but the suitable ones were not obtained. From the Jacobian matrix (set II) exhibited in Table 14, h_1^{o-ca-o} gives certain influences on the molecular vibrations $\nu_1(B_u)$, $\nu_2(A_u, E_g)$ and $\nu_4(E_g)$, the translatory vibrations A_u (180 cm^{-1}), B_g (210 cm^{-1}) and E_u (143 cm^{-1}) and the rotatory vibrations A_u (213 cm^{-1}). The physical meaning of h_1^{o-ca-o} with the negative value is ambiguous. In the case of the set II, the weighed sum of squared deviations S is 0.00327 and the average frequency deviation is $2.8\,{}^0\!/_0$. As is shown in Table 15, the force constants of the set II, fitting best for the lattice vibrations, explain also the magnitude of the frequency splittings of intramolecular vibrations.

It is an important result for this study that the determined force constants are physically reasonable and follow the reasonable trends with respect to the molecular parameters. For example, it would be *of scheelite in* Å/mdyn · sec^2

$f_1(O\cdots O)$	$f_2(O\cdots O)$	$f_3(O\cdots O)$	$f_4(O\cdots O)$	$f_5(O\cdots O)$	$f_1(Ca\cdots W)$	$f_2(Ca\cdots W)$	$f(Ca\cdots Ca)$	$\varkappa$	$p(W-O, W-O)$
0.247	0.154	0.090	0.049	0.021	0.161	0.065	0.032	0.021	0.493
0.010	*0.026*	*0.007*	*0.220*	0.023	0.000	0.000	0.000	0.000	0.187
0.042	*0.000*	*0.042*	*−0.005*	0.019	0.000	0.000	0.000	0.000	0.187
0.016	*0.150*	*−0.003*	0.020	*0.041*	0.000	0.000	0.000	−0.018	0.000
0.085	*0.000*	*0.136*	0.015	*0.006*	0.000	0.000	0.000	−0.017	0.000
0.003	*0.206*	*0.051*	0.013	0.101	0.000	0.000	0.000	−0.012	0.000
0.159	*0.000*	*−0.004*	0.017	0.061	0.000	0.000	0.000	−0.012	0.000
0.010	*0.025*	*0.035*	*0.201*	0.023	0.000	0.000	0.000	0.000	−0.069
0.041	*0.000*	*0.007*	*−0.005*	0.017	0.000	0.004	0.000	0.000	−0.069
0.039	*0.022*	0.019	*0.200*	0.000	0.000	0.000	0.000	0.000	−0.070
0.010	*0.000*	0.023	*−0.005*	0.000	0.000	0.000	0.000	0.000	−0.070
0.002	*0.019*	*0.123*	0.009	*0.011*	0.000	*0.006*	*0.029*	0.032	0.000
0.004	*0.000*	*−0.003*	0.005	*0.052*	0.000	*0.061*	*0.000*	0.039	0.000
0.136	*0.134*	0.028	0.004	0.000	0.000	0.000	0.000	0.046	0.000
0.002	*0.000*	0.020	0.006	0.000	0.000	0.000	0.000	0.050	0.000
0.012	0.000	0.000	0.012	0.008	0.000	0.058	0.161	0.007	0.000
0.009	0.016	0.020	0.005	0.000	0.048	0.014	0.070	0.000	0.000
0.025	0.000	−0.003	0.005	0.013	0.000	0.000	0.000	0.002	0.000
0.009	0.000	0.058	0.006	0.000	0.013	0.006	0.000	0.000	0.000
0.009	0.009	0.000	0.024	0.000	0.002	0.010	0.005	0.003	0.000
0.004	0.000	0.023	0.012	0.001	0.000	0.000	0.025	0.002	0.000
0.028	0.069	0.065	0.004	0.000	0.009	0.004	0.016	0.000	0.000
0.005	0.073	0.000	−0.006	0.066	0.000	0.000	0.000	−0.002	0.000
0.092	0.000	0.060	0.000	0.106	0.000	0.000	0.000	−0.004	0.000
0.000	0.000	0.030	0.003	0.000	0.047	0.021	0.000	0.000	0.000

expected that as the Ca—O distance decreases, the corresponding interaction force constants would increase. The Ca—O distance of r_1(Ca—O) is smaller than that of r_2(Ca—O) and the obtained force constant of $k_1^{\mathrm{ca-o}}$ is larger than that of $k_2^{\mathrm{ca-o}}$. Thus, the expected trend is followed in a qualitative manner. This trend is also satisfactorily kept in the case of the tungsten$\cdots$calcium interaction ($f_1^{\mathrm{ca\cdots w}} = 0.16$ corresponding to $q_1^{\mathrm{ca\cdots w}} = 3.707$ and $f_2^{\mathrm{ca\cdots w}} = 0.07$ mdyn/Å corresponding to $q_2^{\mathrm{ca\cdots w}} = 3.868$ Å).

Table 15. *Frequency splittings of scheelite*

	$\Delta\nu_{\mathrm{obs}}$	$\Delta\nu_{\mathrm{calc}}$
ν_1 (A_g, B_u)	19 cm^{-1}	15 cm^{-1}
ν_2 (A_g, B_u)	24	35
ν_2 (B_g, A_u)	34	30
ν_3 (B_g, A_u)	60	21
ν_3 (E_g, E_u)	4	11
ν_4 (B_g, A_u)	99	88
ν_4 (E_g, E_u)	100	103

Table 16. *Short-range oxygen · · · oxygen distances and force constants in scheelite*

	Interatomic distance	Force constant
q_1	2.767 Å	0.247 mdyn/Å
q_2	2.874	0.154
q_β	2.880	0.142
q_3	2.938	0.090
q_α	2.985	0.071
q_4	3.036	0.049
q_5	3.142	0.021

It was pointed out by Levitt (1969) that with decrease of the bond angles without any change between the bond distance the bond orbitals more and more increase overlapping. Thus, it is more difficult to give distortion for a smaller angle from its equilibrium position than for a larger angle. For this reason, as the angles decrease the bending-force constants should increase in magnitude. This tendency is really revealed in the bending-force constant H with change in O—W—O angle, as is conspicuous in Table 12.

The non-bonded force constants increase with decreasing of the non-bonded distance, as is shown in Table 16. Since the number of electrons about the nucleus of oxygen is intermediate between those about that of Ne and Ar, the repulsion forces for a given O... O distance is expected to be intermediate between those for Ne and Ar. From the data of Fowler and Guggenheim (1949), the constants A and B in the equation (7) are 34.9 mdyn · Å^7 and 55,380 mdyn · Å^{13}

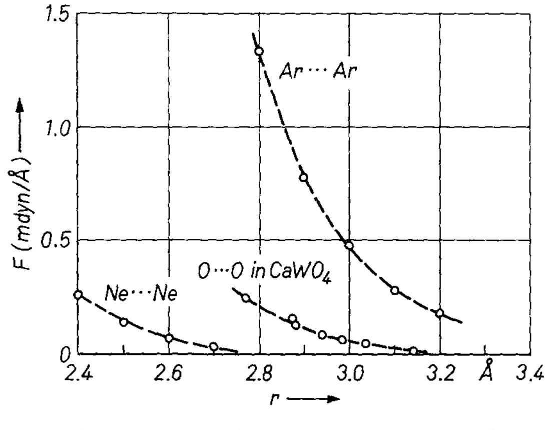

Fig. 5. Non-bonded oxygen · · · oxygen forces

for Ne and 432.6 mdyn · Å^7 and 2,527,000 mdyn · Å^{13} for Ar, respectively. As expected, the O···O curve falls between those for Ne···Ne and Ar···Ar, as is obvious in Fig. 5. The determined values of repulsive-force constant of non-bonded oxygen atom in the present study are thus quite reasonable with regard to previous values for similar systems.

As has been stated above, all of the obtained values for the stretching, bending and non-bonded force constants seem of a reasonable magnitude and qualitatively allow the expected trends.

As the next step, the frequency splitting (Table 15) and the lattice vibrations (Table 13) are physically interpreted on the basis of the frequency mode (Figs. 6, 7 and 8) introduced from L_{xm} matrix and the Jacobian matrix (Table 14).

The observed magnitude of splitting for the totally symmetric stretching (ν_1) is estimated 19 cm^{-1}. The calculated values of ν_1 are 909 (A_g) and 894 cm^{-1} (B_u), the magnitude of its splitting being 15 cm^{-1}. The coincidence of the calculated values with the observed ones is satisfactory. As is clear from the Jacobian matrix in Table 14, this splitting is mainly attributed to the intermolecular O···O repulsion and the O—Ca—O deformation. Here, it is also important that the value of $h_1^{\mathrm{o-ca-o}}$ is negative. This splitting is clearly understood by inspecting the modes of vibration indicated in Fig. 6.

The calculated values of ν_3 are 774 cm^{-1} (A_u) and 795 cm^{-1} (B_g) as well as 800 cm^{-1} (E_g) and 789 cm^{-1} (E_u), the magnitude of their splitting being estimated 21 and 11 cm^{-1} respectively. The corresponding observed values are 60 and 4 cm^{-1}. The calculated values coincide with the observed ones unsatisfactorily for the former splitting but fairly well for the latter. The degree of the observed splitting of $\nu_3(A_u)$ and $\nu_3(B_g)$ of $\nu_3(E_g)$ and $\nu_3(E_u)$ cannot be explained through reference to only the intermolecular interactions. Such a large magnitude of splitting between 778 cm^{-1} (A_u) and 834 cm^{-1} (B_g) in scheelite, the ionic crystal, is therefore attributed presumably to the appreciable amount of the electrostatic force. This electrostatic force is considered to be caused by a macroscopic polarization due to an in-phase displacement of the ions in the crystal (A_u-type), being not involved in the infrared inactive B_g-type vibrations. This situation is obviously shown in the mode of vibration of A_u(778 cm^{-1}) and B_g(838 cm^{-1}).

The calculated values of ν_2 are 332 cm^{-1} (A_g) and 367 cm^{-1} (B_u) together with 400 cm^{-1} (B_g) and 430 cm^{-1} (A_u), the magnitude of splitting being 35 and 30 cm^{-1}. The corresponding values observed

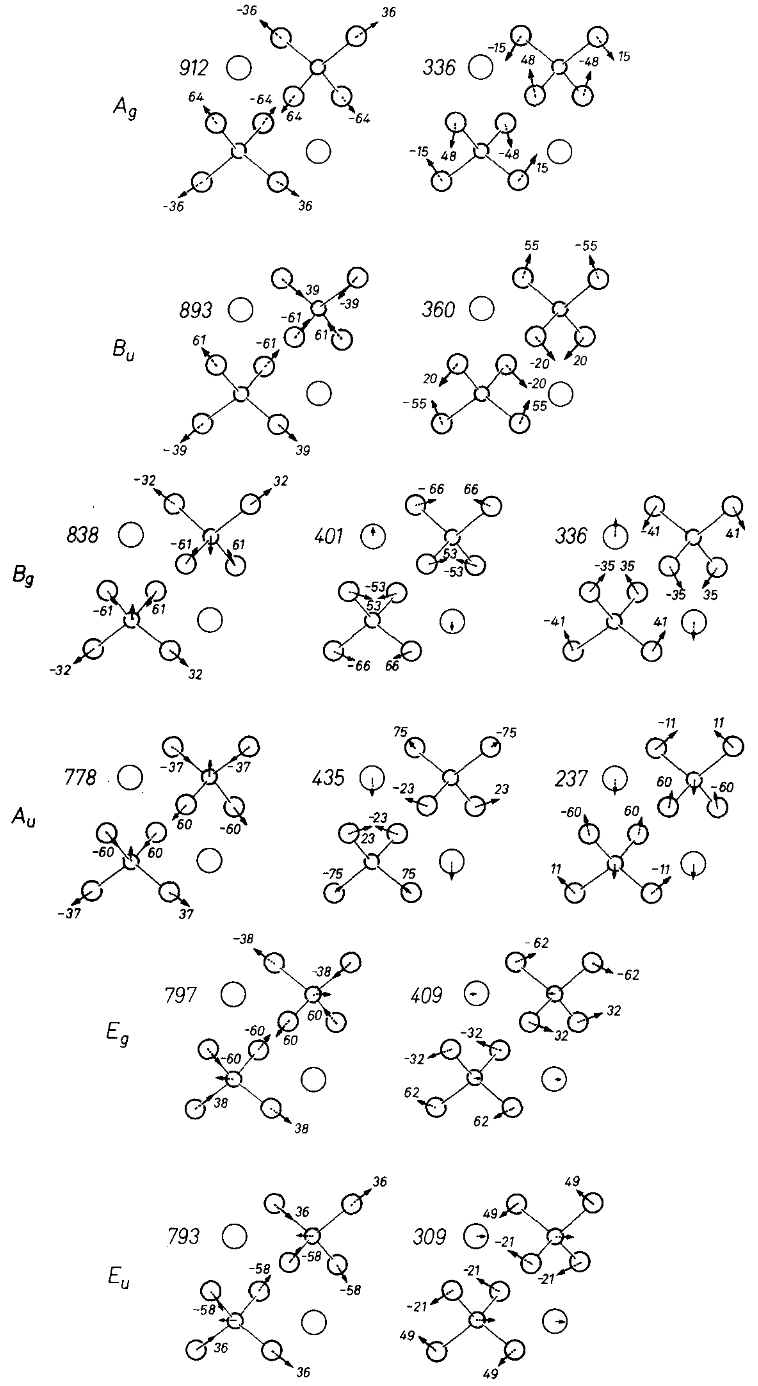

Fig. 6. The "internal" modes of vibration of scheelite

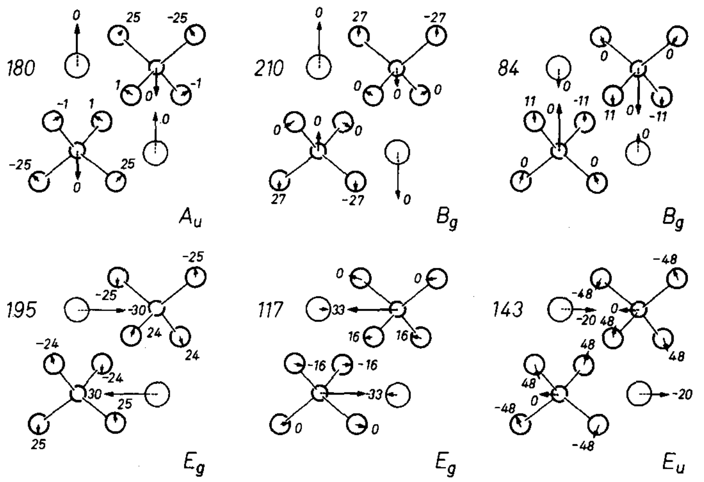

Fig. 7. The "external" modes of vibration of scheelite (translatory)

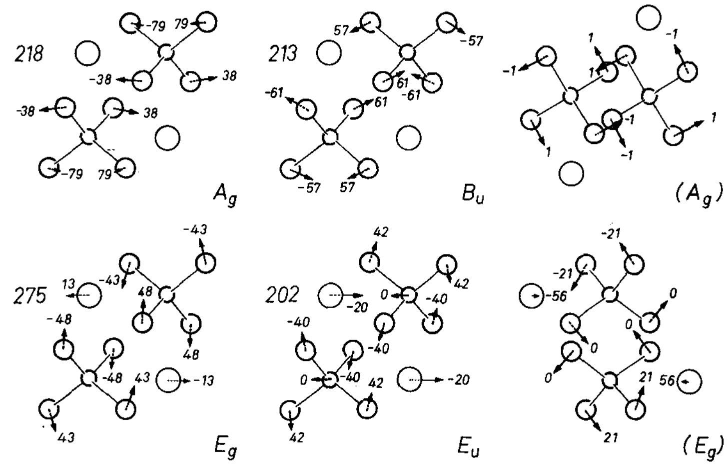

Fig. 8. The "external" modes of vibration of scheelite (rotatory)

are 24 and 34 cm^{-1}. Both cases for splitting are mainly in connection with different effect of the intermolecular potential caused by vibrations (see Fig. 6). In other words, $f_1^{\text{o}\cdots\text{o}}$, $k_1^{\text{ca-o}}$ and $k_2^{\text{ca-o}}$ have large effect on the infrared active vibrations B_u and A_u on one hand and $f_2^{\text{o}\cdots\text{o}}$ on the Raman active vibrations A_g and B_g on the other.

Of all the intramolecular vibrations, the asymmetric WO_4 stretching and deformation vibration (ν_4) shows the largest splitting. The observed values of frequency for ν_4 are 336 cm^{-1} (B_g) and 237 cm^{-1} (A_u) as well as 409 cm^{-1} (E_g) and 309 cm^{-1} (E_u). The degree of splitting in both cases is very conspicuous (estimated about 100 cm^{-1}) and their calculated values also scatter largely. Concord of the calculated values with the observed ones is marked. The large-scaled splitting of ν_4 is also ascribed to the intermolecular interactions. The intermolecular forces $k_1^{\mathrm{ca-o}}$, $f_2^{\mathrm{o\cdots o}}$, $f_3^{\mathrm{o\cdots o}}$ largely affect on $B_g(\nu_4)$, while the intermolecular force $h_1^{\mathrm{o-ca-o}}$ yields the negative effect on $A_u(\nu_4)$. $B_g(\nu_4)$ frequency is thus estimated 100 cm^{-1} in magnitude larger than that for $A_u(\nu_4)$. The large splitting between $E_g(\nu_4)$ and $E_u(\nu_4)$ is brought about intensely by the intermolecular interaction forces $f_1^{\mathrm{o\cdots o}}$ and $f_2^{\mathrm{o\cdots o}}$, as is obviously deducible from the Jacobian matrix (Table 14) and the modes of vibration (Fig. 6).

The data of the observed and calculated values for the external vibrations are in excellent harmony with each other, as is given in Table 13. As is clear from the Jacobian matrix, all of the observed values for frequency are principally enlightened after the reasonable set of the intermolecular interaction forces between oxygen$\cdots$oxygen, tungsten$\cdots$calcium, calcium$\cdots$calcium and calcium—oxygen. But the intramolecular force constants give certain effects on the lattice vibrations, *i.e.*, the rotational and translational lattice vibrations are not perfectly separatable from the intramolecular vibrations in this crystal. This is also clear from the modes of vibration, as is revealed in Figs. 7 and 8.

The translatory external vibrations are dividable into two parts, of which one is translatable parallel to z axis (A_u and B_g) and the other parallel to x or y axis (E_g and E_u, degenerate). Calcium ions translate chiefly in the translatory lattice vibrations A_u(180 cm^{-1}), B_g(210 cm^{-1}), E_g(195 cm^{-1}) and E_u(143 cm^{-1}) and tungaten atoms largely in the translatory lattice vibrations B_g(84 cm^{-1}) and E_g(117 cm^{-1}). The atomic weight of tungsten atom is larger than that of calcium. It is considered that this is the reason why 84 cm^{-1} and 117 cm^{-1} vibrations bear the values of frequency smaller than those of the other translational external vibrations. Differences in frequency between A_u(180 cm^{-1}) and B_g(210 cm^{-1}) is combined with the effects of the intermolecular interaction forces $k_2^{\mathrm{ca-o}}$, $f_1^{\mathrm{ca\cdots w}}$ and $f^{\mathrm{ca\cdots ca}}$, being clearly understood by examining the modes of vibration and the Jacobian matrix.

As is shown in Fig. 8, the rotational external vibrations A_g(218 cm^{-1} and B_u(213 cm^{-1}) are recognized to rotate about the z axis and the degenerate rotational external vibrations E_g(275 cm^{-1}) and E_u(202 cm^{-1}) about the x or y axis. The difference in the frequency is explained by the Jacobian matrix and the modes of vibration. The force constants $k_2^{\text{ca-o}}$, $f_1^{\text{o}\cdots\text{o}}$ and $f_2^{\text{o}\cdots\text{o}}$ give the remarkable effects only on E_g and $f_1^{\text{ca}\cdots\text{w}}$ and $f_2^{\text{ca}\cdots\text{w}}$ on E_u. The former effect is more conspicuous than the latter, resulting in the large difference in frequency between E_g(275 cm^{-1}) and E_u(202 cm^{-1}). On the other hand, difference in frequency between A_g(218 cm^{-1}) and B_u(213 cm^{-1}) is small in magnitude. In this case, the force constants $k_1^{\text{ca-o}}$, $k_2^{\text{ca-o}}$ and $f_2^{\text{o}\cdots\text{o}}$ give the intense effects on A_g(218 cm^{-1}) and all of the other force constants on B_u(213 cm^{-1}), eventuating in small difference of frequency.

Acknowledgements

The writer wishes to express his sincere gratitude to Prof. Y. UMEGAKI of Hiroshima University for his kind advice and critical reading of the manuscript, to Assistant Prof. Y. SHIRO of the same University for his stimulating and helpful discussions.

References

A. S. BARKER, JR. (1964), Infrared lattice vibrations in calcium tungstate and calcium molybdate. Physic. Rev. **135**, 742—747.

R. H. BUSEY and O. L. KELLER, JR. (1964), Structure of the aqueous pertechnetate ion by Raman and infrared spectroscopy. Raman and infrared spectra of crystalline $KTcO_4$, $KReO_4$, Na_2MoO_4, Na_2WO_4, $Na_2MoO_4 \cdot 2H_2O$, and $Na_2WO_4 \cdot 2H_2O$. J. Chem. Physics **41**, 215—225.

J. P. DEVLIN (1963), Urey-Bradley nonbonded forces. J. Chem. Physics **39**, 2385.

J. P. DEVLIN (1964), Urey-Bradley nonbonded forces, II. J. Chem. Physics **41**, 2951—2952.

R. FOWLER and E. A. GUGGENHEIM (1949), *Statistical thermodynamics*. Cambridge University Press, Cambridge.

M. I. KAY, B. C. FRAZER and I. ALMODOVAR (1964), Neutron diffraction refinement of $CaWO_4$. J. Chem. Physics **40**, 504—506.

R. K. KHANNA, W. S. BROWER, B. R. GUSCOTT and E. R. LIPPINCOTT (1968), Lazer induced Raman spectra of some tungstates and molybdates. J. Res. Natl. Bur. Stand. **72 A**, 81—84.

S. R. LEVITT (1969), *The vibrational spectroscopy and normal coordinate analysis of geological apatites*. Ph. D. Thesis, S. U. N. Y., College of Ceramics, Alfred University. Alfred, New York 14802.

D. E. MANN, L. FANO, W. F. CAHILL, and T. SHIMANOUCHI (1954), The application of a high-speed digital computer to molecular vibration problems. J. Chem. Physics **22**, 764.

A. MÜLLER and B. KREBS (1967), Normal coordinate treatment of XY_4-type molecules and ions with T_d symmetry. Part I. Force constants of a modified valence force field and of the Urey-Bradley force field. J. Molec. Spectr. **24**, 180—197.

S. P. S. PORTO and J. F. SCOTT (1967), Raman spectra of $CaWO_4$, $SrWO_4$, $CaMoO_4$ and $SrMoO_4$. Physic. Rev. **157**, 716—719.

J. P. RUSSELL and R. LOUDON (1965), The first-order Raman spectrum of calcium tungstate. Proc. Physic. Soc. [London] **85**, 1029—1033.

J. F. SCOTT (1968*a*), Lattice perturbations in $CaWO_4$ and $CaMoO_4$. J. Chem. Physics **48**, 874—876.

J. F. SCOTT (1968*b*), Dipole-dipole interactions in tungstates. J. Chem. Physics **49**, 98—100.

T. SHIMANOUCHI (1963), Force constants of small molecules. Pure Appl. Chem. **7**, 131—145.

T. SHIMANOUCHI and I. SUZUKI (1964), Method of adjusting force constants and its application to H_2O, H_2CO, CH_2Cl and their deuterated molecules. J. Chem. Physics **42**, 296—308.

A. ZALKIN and D. H. TEMPLETON (1964), X-ray diffraction refinement of the calcium tungstate structure. J. Chem. Physics **40**, 501—504.